

# A Density Functional Theory Study to Analyze the Inhibition Potential of Some Antidepressant Molecules on Metal Corrosion in Acidic Media

Mougo André Tigori<sup>1</sup>, Yeo Mamadou<sup>2</sup>, N'guadi Blaise Allou<sup>2</sup>, Paulin Marius Niamien<sup>2</sup>

<sup>1</sup>Laboratoire des Sciences et Technologies de l'Environnement, UFR Environnement, Université Jean Lorougnon Guédé, BP 150 Daloa, Côte d'Ivoire

<sup>2</sup>Laboratoire de Constitution et de Réaction de la Matière, UFR SSMT, Université Félix Houphouët-Boigny, 22 BP 582 Abidjan 22, Côte d'Ivoire

Correspondence: Mougo André Tigori, UFR Environnement, Université Jean Lorougnon Guédé, BP 150 Daloa, Côte d'Ivoire. E-mail: [tigori20@yahoo.fr](mailto:tigori20@yahoo.fr)

Received: February 19, 2023 Accepted: March 30, 2023 Online Published: April 2, 2023

doi:10.5539/ijc.v15n1p31

URL: <https://doi.org/10.5539/ijc.v15n1p31>

## Abstract

The use of therapeutic molecules in corrosion inhibition field contributes to environment preservation. In this context that this current work applies quantum chemical method to study the interaction between some metals and four compounds with antidepressant effect. Which compounds are clomipramine, imipramine, amoxapine and iproniazide. The inhibition properties of these compounds in acidic media were evaluated by density functional theory (DFT) with B3LYP functional in 6-31G(d,p) basis set. It was proved that these compounds have a strong electron donating and accepting capacity. This capacity is influenced by their substituents. The low energy gap ( $\Delta E$ ) values obtained denote that these molecules are highly reactive and can form coordination bonds for the establishment of a barrier on metal surface that could reduce corrosion process. Reactivity sites prediction were carried out by Fukui functions ( $f_k^+$ ,  $f_k^-$ ) and dual descriptor ( $\Delta f_k(r)$ ), it appears that the centers of nucleophilic attacks are in general nitrogen (N) atoms whereas the centers of electrophilic attacks are only carbon atoms (C).

**Keywords:** therapeutic molecules, therapeutic molecules, metals, density functional theory, reactivity sites

## 1. Introduction

Density functional theory (DFT) based on quantum chemical was originally developed and applied to solid state problems, has currently become a very important tool to explain the behavior of molecular systems and chemical problems (Ziegler, 1991; Bochuan *et al.*, 2018; Nurudeen *et al.*, 2022). Indeed in recent years, DFT has permitted to correlate the inhibition efficiency of some organic compounds to their molecular structures (Zarrouk *et al.*, 2013; Danaee *et al.*, 2013; Lazrak *et al.*, 2022; Yue *et al.*, 2018). It has been proved that this correlation is attributed to the molecular structure of the compounds, for example, the mobility and presence of lone electrons in the heteroatoms, which are important characteristics determining, the adsorption capacity of an organic compound (Ambrish *et al.*, 2018; Priyanka *et al.*, 2016; Abd El-Maksoud *et al.*, 2021). The adsorption on metal surface depends on the inhibitor electronic structure, while the type of interaction between metal surface and the molecular structure influences the inhibition efficiency (Tigori *et al.*, 2022; Khaled, 2008). The use of quantum chemical in corrosion field has led to the understanding that many organic compounds containing conjugated double bonds, groups with heteroatoms (N, S, O) and polar functional groups can be used as corrosion inhibitors (Jing *et al.*, 2016; Loganathan *et al.*, 2021; Jian *et al.*, 2018; Cher *et al.*, 2020). Metal equipment corrosion is one of the main industrial problems because, it is associated with significant safety problems, environmental pollution and economic losses. Therefore, the non-toxic and inexpensive environmental inhibitors are sought to reduce the damage caused by corrosion in acidic solutions (Dehghani *et al.*, 2019; Lanzhou *et al.*, 2020; Mohanapriya *et al.*, 2020). In the search for non-toxic corrosion inhibitors, many authors in this field attest that drugs are alternative molecules that have almost the same properties as green corrosion inhibitors, they have negligible negative effects on the environment, they are generally non-toxic, cheap and accessible (Adejoro *et al.*, 2016; Žaklina *et al.*, 2018; Palaniappan *et al.*, 2019; Ileana *et al.*, 2014; Sumayah *et al.*, 2018).

Therefore, the purpose of the present work is to study theoretically the inhibition potentials of four compounds with antidepressant effect for metals such as iron, aluminium and copper corrosion in acid medium using DFT method. These compounds are Clomipramine, Imipramine, Amoxapine and Iproniazide. This theoretical approach will consist in studying the influence of substituents in these molecules reactivity. The choice of the acidic medium is justified by the

fact that acidic solutions are commonly used for certain operations such as acid pickling, acid cleaning and chemical or electrochemical etching which often consist in removing corrosion products on metal equipment. Thus, to reduce the dissolution of metals exposed to these aggressive solutions during the different operations, it is necessary to add corrosion inhibitors.

## 2. Experimental

### 2.1 Molecular Depiction

The molecules used as inhibitors in this study are drugs to fight depression. Their molecular structure is given by Figure 1.

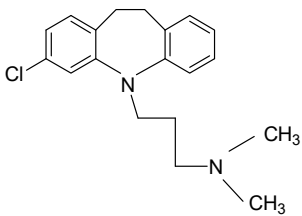
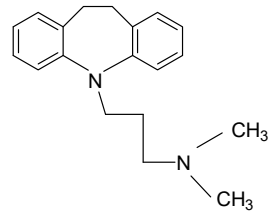
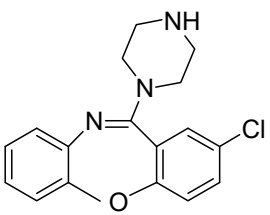
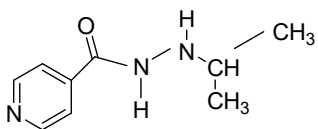
Name	Molecular structure
3-(3-chloro-10,11-dihydro-5H-dibenzo[b,f]azepin-5-yl)-N,N-dimethylpropan-1-amine or clomipramine (CPA)	
10,11-dihydro-N,N-dimethyl-5H-dibenz-[b,f]azepin-5-panamine or Imipramine (IPA)	
8-chloro-6-piperazin-1-ylbenzo[b][1,4]benzoxazepine or Amoxapine (AP)	
N'-propan-2-ylpyridine-4-carbohydrazide or Iproniazide (IZ)	

Figure 1. Molecular structures of CPA, IPA, AP and IZ

### 2.2 Density Functional Theory (DFT) Calculations Details

In order to study the organic molecules reactivity and the relationship between the molecular structure and inhibition performance of studied molecules, quantum chemical calculations were performed. The different calculations in this study were carried out by Density Functional Theory (DFT) with the program Gaussian 09W (Frisch *et al.*, 2009). Indeed DFT provides a main theoretical basis for the calculation of energy band structure (Vandana *et al.*, 2020). The fundamental idea is that the exact properties of the ground state of a closed system, i.e. without chemical reactions, formed by nuclei positioned in fixed sites and electrons surrounding them, are functionals of the electron density alone (Hohenberg *et al.*, 1964). Thus, the energy of electronic device is given by:

$$E[\rho] = V_{ext}[\rho] + T_S[\rho] + J[\rho] + E_{xc}[\rho] \quad (1)$$

$V_{ext}$ : external potential;

$T_S$ : kinetic energy of the fictitious system;

$J$ : coulombic repulsion;

$E_{xc}$ : energy of exchange correlation. This energy is determined from the Local Density Approximation (LDA) and Generalized Gradient Approximation (GGA).

The optimization of geometries molecules was performed with Gaussview 5.0 Software. In this theory, B3LYP functional (Lee, Yang and Parr's 3-parameter hybrid functional) was used to establish the necessary relationships between density and energy (Becke, 1992; Lee *et al.*, 1988). This functional is commonly used for its good accuracy in a wide range of molecular properties. The basis used to describe the atomic orbitals and construct the molecular orbitals is 6-31G(d,p). It was used for its good accuracy in the calculations and in order to obtain better results for optimization geometries. These calculations provided access to the highest occupied molecular orbital energy ( $E_{HOMO}$ ), the lowest unoccupied molecular orbital energy ( $E_{LUMO}$ ), energy gap ( $\Delta E$ ), dipole moment ( $\mu$ ), electron affinity (A), ionization energy (I), electronegativity ( $\chi$ ), hardness ( $\eta$ ), softness ( $\sigma$ ), electrophilicity index ( $\omega$ ), global electron donating power, ( $\omega^-$ ), global electron accepting power ( $\omega^+$ ), net electrophilicity ( $\Delta\omega^\pm$ ), fraction of electron transferred ( $\Delta N$ ), total energy ( $E_T$ ), Fukui functions ( $f_k^+$ ,  $f_k^-$ ) and dual descriptor ( $\Delta f_k(r)$ ).

### 3. Results and Discussion

#### 3.1 Global Reactivity Inhibitors Analysis

The values of quantum chemical parameters permitting to study the compounds reactivity are displayed in Table 1. These parameters were determined by DFT/B3LYP in 6-31G (d,p) basis set.

Table 1. Quantum chemical parameters of studied compounds

Parameters	CPA	IPA	AP	IZ
$E_{HOMO}$ (eV)	-4.6251	-4.8544	-5.2988	-6.7673
$E_{LUMO}$ (eV)	-1.1848	-0.7192	-1.3015	-1.3978
Energy gap $\Delta E$ (eV)	3.4403	4.1352	3.9973	5.3695
Dipole moment $\mu$ (D)	3.4312	3.7811	1.1067	2.8571
Total energy $E_T$ (Ha)	-1307.4727	-1307.68130	-1357.1196	-590.2600

In accordance with the frontier molecular orbitals theory (FMO), HOMO and LUMO energy levels determine the ability of inhibitor molecules to gain and lose electrons. Indeed, according to literature the higher the HOMO energy of inhibitor, the greater the tendency to offer electrons to metal and the lower its  $E_{LUMO}$  energy, the more readily the molecule accepts electrons from the metal (Rahmani *et al.*, 2019; Khattabi *et al.*, 2019).  $E_{HOMO}$  and  $E_{LUMO}$  energies of the four compounds studied are listed in Table 1. It is apparent that  $E_{HOMO}$  values obtained are high, so the compounds studied have a good ability to provide electrons to the metal. During corrosion, the metal loses electrons. This ability of the studied compounds to give electrons to the metal will participate in the formation of a protective layer strongly linked to metal surface, effectively preventing its oxidation.  $E_{LUMO}$  values obtained during this study are low for each molecules thus marking the aptitude of these compounds to acquire electrons. The energy of these two orbitals is directly related to the adsorption type of each molecule on metal surface. The electrons that are mainly distributed on the oxygen and nitrogen atoms contained in each compound, are more likely to donate lone pairs to empty metal orbitals to form covalent bonds. The formation of these bonds promotes chemical adsorption which indicates the good inhibition performance of the studied compounds.

Energy gap were computed from the following equation (Tengda *et al.*, 2021)

$$\Delta E = E_{LUMO} - E_{HOMO} \quad (2)$$

Energy gap of studied molecules are between 3.44 and 5eV and are in the following order:  $\Delta E(CPA) < \Delta E(AP) < \Delta E(IPA) < \Delta E(IZ)$ , which according to previous studies are low values (Vranda *et al.*, 2021; Dehghani *et al.*, 2019; Bahlakeh *et al.*, 2019). These low values attest that CPA, AP, IPA and IZ molecules are unstable because they possess a strong electron donating ability. Therefore they can react with the metal to form coordination bonds. The formation of these covalent bonds reduce metals corrosion (Sourav *et al.*, 2015). In fact covalent bonds formation strengthens metal surface in electrons. Thus the electrons that metal loses during its oxidation are replaced by the establishment of these covalent bonds. Energy gap evolution per inhibitor is related by Figure 2. This evolution indicates that CPA and AP have the lowest  $\Delta E$  values. Analysis of these values reveals that CPA and AP which have chlorine in their molecular structure

are more reactive than the other compounds studied, it follows that the position of chlorine in CPA and AP favors electronic exchanges within the molecule. These exchanges will create electronegative groups with lone electron pairs and  $\pi$  electrons of conjugated double bonds that will serve to form covalent bonds with the metal. In light of the following, CPA and AP may have the best inhibition properties than the other compounds studied.

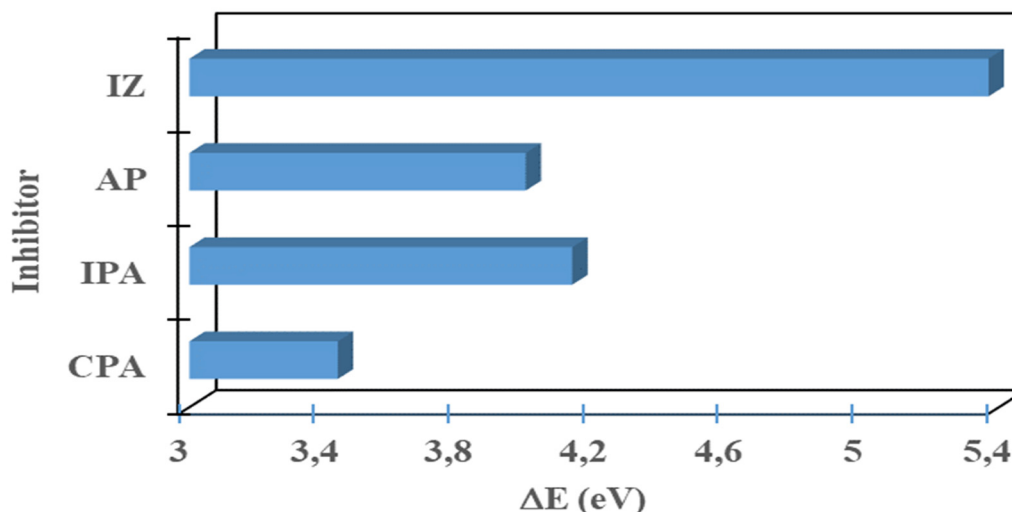


Figure 2.  $\Delta E$  Evolution per inhibitor

The correlation between dipole moment ( $\mu$ ) and inhibition efficiency of compounds is variously interpreted by several authors (Rajesh *et al.*, 2018; Pavithra *et al.*, 2013; Soltani *et al.*, 2015). In fact some authors suggest that an increase in the dipole moment leads to a decrease in the inhibition efficiency. According to some authors, lower values of the dipole moment will favor the accumulation of the inhibitor on metal surface, while others believe that the opposite is true. In our study the values obtained oscillate between 1.10 D and 3.80 D. By comparing these values to those obtained in the literature, the molecules studied can adsorb to metal surface (Zarrouk *et al.*, 2014).

Total energies are negative, this implies that the transfer of electrons from the inhibitors to the metal is very favorable (Tigori *et al.*, 2020).

The quantum chemical parameters values from DFT conceptual were listed in table 2.

Table 2. Quantum chemical parameters from DFT conceptual

Parameters	CPA	IPA	AP	IZ
Ionization energy $I$ (eV)	4.6251	4.8544	5.2988	6.7673
Electron affinity $A$ (eV)	1.1848	0.7192	1.3015	1.3978
Electronegativity $\chi$ (eV)	2.9050	2.7868	3.3001	4.0826
Hardness $\eta$ (eV)	1.7202	2.0676	1.9987	2.6848
Softness $\sigma$ (eV) <sup>-1</sup>	0.5813	0.4837	0.5003	0.3725
Electrophilicity index $\omega$	2.4530	1.8781	2.7245	3.1041
Electroaccepting power $\omega^+$	1.2154	0.8932	1.5386	2.1825
Electrodonating power $\omega^-$	4.1204	4.2429	5.3732	8.5544
Net electrophilicity $\Delta\omega^\pm$	4.3358	5.1361	6.9118	10.7369

Electron density distribution of HOMO and LUMO orbitals for each molecule is shown in Figure 3. Examining this Figure, it is apparent that electrons are mainly distributed on heteroatoms (N,O) and carbon-carbon double bonds (C=C) at aromatic rings. This distribution indicates that heteroatoms and (C=C) bonds at aromatic rings are more likely to donate lone pairs to empty metal orbitals to form covalent bonds. It is also observed that for the same molecule, HOMO and LUMO distributions are almost in the same part. These observations relate that the parts containing the heteroatoms and the aromatic rings in these compounds are the seat of the electron donation and acceptance.

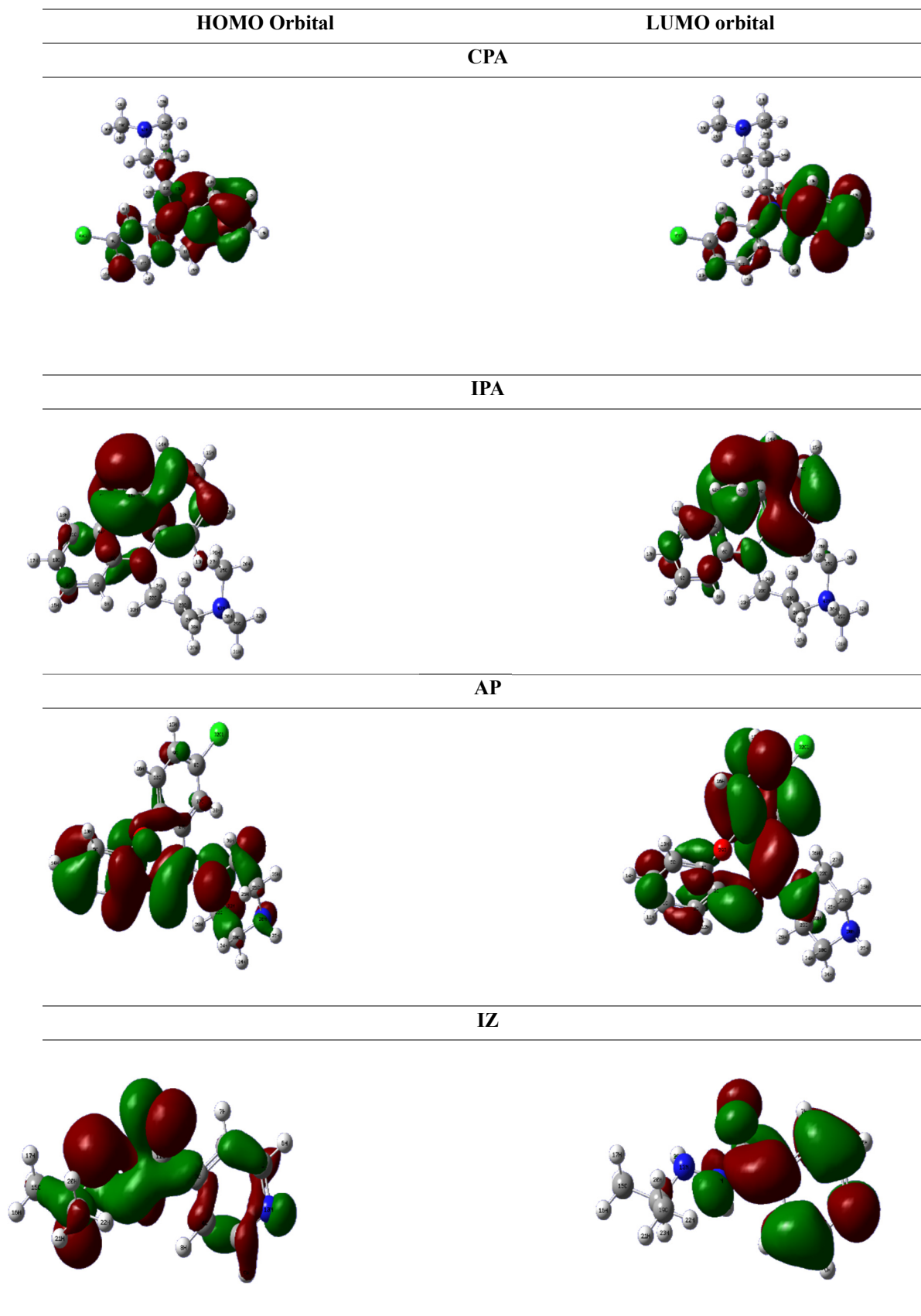


Figure 3. HOMO and LUMO electron density distribution

Ionization potential ( $I$ ) is attached to highest occupied molecular orbital energy ( $E_{HOMO}$ ) (Kurks et al., 2021), it reflects the ability to donate electrons while the electron affinity ( $A$ ) which depends to the lowest unoccupied molecular orbital energy ( $E_{LUMO}$ ) implies the tendency to accept electrons (Lukman et al., 2016; Zhang et al., 2021). They are expressed as follows:

$$I = -E_{HOMO} \quad (3)$$

$$A = -E_{LUMO} \quad (4)$$

The values of these parameters for studied molecule are listed in Table 2. These values describe the donor and acceptor character of these compounds. This character ensures them a good inhibition potentiality in a metal corrosion.

Global hardness ( $\eta$ ) and softness ( $\sigma$ ) predict an organic compound reactivity (Vranda et al., 2021). These parameters are determined by the following relationships:

$$\eta = \frac{I-A}{2} \quad (5)$$

$$\sigma = \frac{1}{\eta} = \frac{2}{I-A} \quad (6)$$

In fact a compound with a high value of  $\eta$  has a high resistance to charge transfer, so it is less reactive, while a molecule that has a high value of  $\sigma$  is highly reactive (Albayati et al., 2020; Behzadi et al., 2015). The values of  $\eta$  and  $\sigma$  obtained in this work compared to that of previous studies attest that the studied compounds are very reactive and will be able to mitigate the corrosion of metals.

Electrophilicity index ( $\omega$ ) introduced by Parr (Parr et al., 1999), reveals the potential of the inhibitor to withdraw electrons from the metal.

$$\omega = \frac{(I+A)^2}{4(I-A)} \quad (7)$$

Electrophilicity index values displayed in Table 2 confirm this capacity of the studied molecules. The property follows the order:  $\omega(\text{IZ}) > \omega(\text{AP}) > \omega(\text{CPA}) > \omega(\text{IPA})$ , confirming the good electron acceptor property of IZ. This property of IZ is due to C=O group presence in this molecule.

Electroaccepting power, electrodonating power and net electrophilicity are calculated from the following equations:

$$\omega^+ = \frac{(I+3A)^2}{16(I-A)} \quad (8)$$

$$\omega^- = \frac{(3I+A)^2}{16(I-A)} \quad (9)$$

$$\Delta\omega^\pm = \omega^+ - (-\omega^-) = \omega^+ + \omega^- \quad (10)$$

CPA, IPA and IZ electroaccepting power ( $\omega^+$ ) values are closer to their calculated electronic affinities ( $A$ ). These values analysis certify that these three compounds have a strong capacity to accept electrons from the metal (José et al., 2007). CPA and IPA have almost similar molecular structures and  $-\text{N}(\text{CH}_3)_2$  group presence in their structure molecular. This presence will contribute to their electron acceptance properties. Indeed two  $-\text{CH}_3$  groups around N atom will stabilize CPA and IPA molecules by inductive donor effect. Thus this N atom will create a deficit of electrons by its electron doublet delocalization. This deficit of electrons created by N atom will be the seat of metal electrons reception. IZ Electron acceptor character is described by C=O group, as confirmed by its electrophilicity index ( $\omega$ ) value.

As for AP compound, its electrodonating power ( $\omega^-$ ) value is closer to Ionization energy ( $I$ ), thus proving its ability to donate electrons to metal (José et al., 2007). This ability is due to several heteroatoms (N and O) presence in this compound.

Net electrophilicity ( $\Delta\omega^\pm$ ) parameter values of studied compounds given in Table 2 are in general close to calculated ionization energy values ( $I$ ), which suggests that these compounds can be protonated in an acidic environment. This possibility of protonation may allow the inhibitors to react with metal to reduce the corrosion process. Similar findings were obtained in the literature (José et al., 2007).

Fraction of electrons transferred ( $\Delta N$ ) is related to molecule and metal electronegativity parameters. It denotes the tendency of electron transfer from the inhibitor molecule to metal atom. This parameter depends on metal type. So, for

this study the fraction of electrons transferred to copper, aluminum and iron was calculated and listed in Table 3.  $\Delta N$  is expressed as follows:

$$\Delta N = \frac{\chi_{\text{metal}} - \chi_{\text{mol}}}{2(\eta_{\text{metal}} + \eta_{\text{inh}})} \quad (11)$$

Where:  $\chi_{\text{Cu}}(\text{eV}) = 4.98$  (Michaelson, 1977),  $\eta_{\text{Cu}} = 0$  (Dewar et al., 1985);  $\chi_{\text{Al}}(\text{eV}) = 4.28$  (Pearson, 1988),  $\eta_{\text{Al}} = 0$  (Maryam et al., 2020);  $\chi_{\text{Fe}}(\text{eV}) = 4.81$  (Tengda et al., 2021),  $\eta_{\text{Fe}} = 0$  (Tengda et al., 2021) and  $\chi_{\text{mol}}$  is electronegativity of studied molecule (Table 2).

An examination of Table 3 reveals that  $\Delta N$  values of different molecules calculated from copper, aluminium and iron electronegativities are all positive and lower than 3.6 ( $\Delta N < 3.6$ ). These results confirm that the inhibitors studied have the ability to donate electrons to metals copper, aluminium and iron. Thus this ability of the molecules to offer electrons reinforces the metal surface which degrades in an acid environment. Therefore CPA, IPA, AP and IZ can be used to inhibit copper, aluminum and iron corrosion.

Similar results with therapeutic molecules have been obtained by Žaklina et al. (Žaklina et al., 2021) and Jabir et al. (Jabir et al., 2016).

Table 3. Fraction of electrons transferred values of studied molecules

Molecule	Metals	$\Delta N$
CPA	Copper	0.6031
	Aluminium	0.3997
	Iron	0.5566
IPA	Copper	0.5304
	Aluminium	0.3611
	Iron	0.4917
AP	Copper	0.4203
	Aluminium	0.2451
	Iron	0.3802
IZ	Copper	0.1671
	Aluminium	0.0368
	Iron	0.1373

### 3.2 Local Molecular Reactivity Study

Global reactivity investigations have reported that the studied molecules are reactive. The good inhibition performances that these compounds possess are due to donation and acceptance of electrons. It is therefore necessary to identify the atoms that are suitable to receive the nucleophilic and electrophilic attacks within each compound. The local reactivity of a corrosion inhibitor is determined by means of Fukui functions (Lianjun et al., 2020) and dual descriptor (Morell et al., 2005; Martínez-Araya, 2015). These local parameters are calculated from the following expressions:

For nucleophilic attack

$$f_k^+ = [q_k(N + 1) - q_k(N)] \quad (11)$$

For electrophilic attack

$$f_k^- = [q_k(N) - q_k(N - 1)] \quad (12)$$

Dual descriptor

$$\Delta f_k(r) = f_k^+ - f_k^- \quad (13)$$

Where  $f_k^+$  and  $f_k^-$  are respectively nucleophilic and electrophilic Fukui functions.  $N$  is the number of electrons in the neutral species, when  $(N + 1)$  corresponds to an anion with an electron added to the LUMO of the molecule and  $(N - 1)$  is the cation with an electron removed from the HOMO the molecule.  $q_k(N + 1)$ ,  $q_k(N)$  and  $q_k(N - 1)$  are the Mulliken charges of the atom  $k$  of the system with  $(N + 1)$ ,  $N$  and  $(N - 1)$  electrons.

Local reactivity parameters values of studied inhibitors are recorded in Tables 4, 5, 6 and 7.

According to the literature, the identification of a site likely to receive a nucleophilic and electrophilic attack is done from the comparison of  $f_k^+$ ,  $f_k^-$  and  $\Delta f_k(r)$  values.

Thus the atom with the highest values of  $f_k^+$  and  $\Delta f_k(r)$  are able to receive a nucleophilic attack in this case the molecule gains electrons, while the atom with the highest value of  $f_k^-$  and the lowest value of  $\Delta f_k(r)$  is likely to receive electrophilic attacks (the molecule loses electrons).

As can be seen from the calculations, local parameter values displayed in Table 4 indicate that C(19) atom is the likely center for nucleophilic attacks, while C(3) carbon is the likely center for electrophilic attacks for CPA. As for the values for IPA listed in Table 5, they reveal that N(21) is the probable site for nucleophilic attacks and C(2) atom is the probable site for electrophilic attacks. Looking at Table 6, it is clear that the probable centers for nucleophilic and electrophilic attacks for AP are N(31) and C(19) atoms, respectively. For IZ, local parameters values in Table 7 relate that N(10) and C(11) are the probable sites for nucleophilic and electrophilic attacks, respectively. These identified atoms are located in red for nucleophilic attack sites and blue for electrophilic attack sites on the optimized structures of each inhibitor in Figure 4. It is a general observation that carbon atoms are more susceptible to electrophilic attack. These carbon atoms share a double bond with other atoms, so these sites are more favorable to donate electrons to metal. On the other hand, the nucleophilic attack sites are usually nitrogen atoms, which release their non-bonding doublet, creating an electron deficit. So these sites become favorable to receive electrons from the metal.

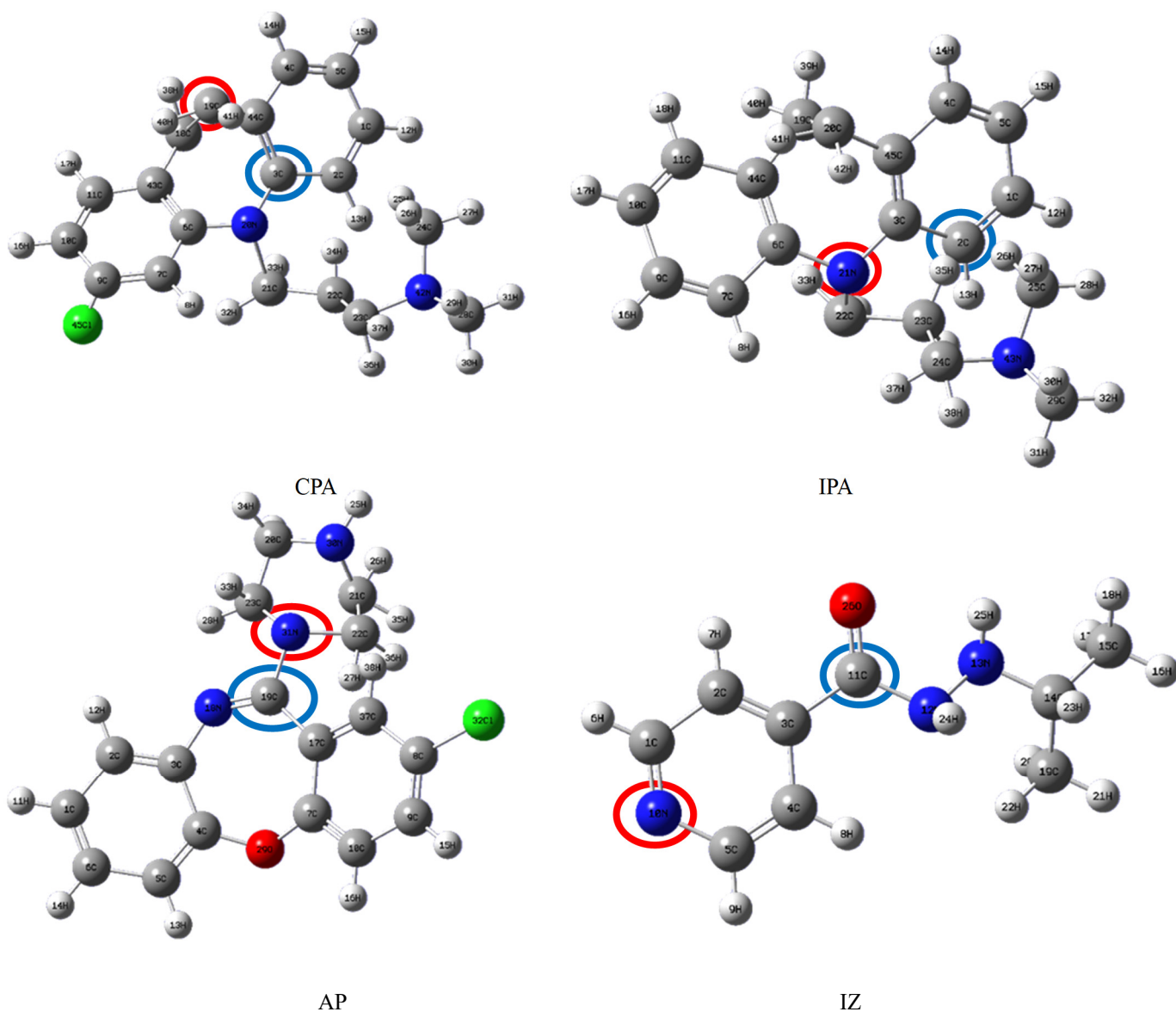




Table 4. Mulliken atomic charges, Fukui function and dual descriptor of CPA by B3LYP/6-31G(d,p)

atoms		$q_k(N + 1)$	$q_k(N)$	$q_k(N - 1)$	$f_k^+$	$f_k^-$	$\Delta f_k(r)$
1	C	0.009767	0.146723	0.237348	-0.136956	-0.090625	-0.046331
2	C	0.028093	-0.105906	0.070833	0.133999	-0.176739	0.310738
<b>3</b>	<b>C</b>	<b>-0.032369</b>	<b>0.31173</b>	<b>0.037936</b>	<b>-0.344099</b>	<b>0.273794</b>	<b>-0.617893</b>
4	C	0.028112	-0.074319	0.269182	0.102431	-0.343501	0.445932
5	C	0.000908	-0.066784	-0.07011	0.067692	0.003326	0.064366
6	C	-0.026306	0.265636	0.021121	-0.291942	0.244515	-0.536457
7	C	0.039247	-0.229219	0.037905	0.268466	-0.267124	0.53559
8	H	-0.001662	0.110543	-0.001935	-0.112205	0.112478	-0.224683
9	C	-0.021458	0.016927	-0.017831	-0.038385	0.034758	-0.073143
10	C	0.046637	-0.228962	0.041791	0.275599	-0.270753	0.546352
11	C	-0.019058	-0.104289	0.018868	0.085231	-0.123157	0.208388
12	H	-0.000315	0.094392	-0.013336	-0.094707	0.107728	-0.202435
13	H	-0.000014	0.155094	-0.004918	-0.155108	0.160012	-0.31512
14	H	0.001647	0.09364	-0.013557	-0.091993	0.107197	-0.19919
15	H	0.000212	0.084432	0.002322	-0.08422	0.08211	-0.16633
16	H	-0.001929	0.132531	-0.002183	-0.13446	0.134714	-0.269174
17	H	0.000595	0.079842	-0.001072	-0.079247	0.080914	-0.160161
18	C	0.000261	-0.302893	0.007411	0.303154	-0.310304	0.613458
<b>19</b>	<b>C</b>	<b>0.862173</b>	<b>-0.362073</b>	<b>0.45867</b>	<b>1.224246</b>	<b>-0.820743</b>	<b>2.044989</b>
20	N	0.134801	-0.590745	-0.016885	0.725546	-0.57386	1.299406
21	C	-0.007105	-0.132209	0.000523	0.125104	-0.132732	0.257836
22	C	0.00962	-0.159847	-0.001016	0.169467	-0.158831	0.328298
23	C	-0.000087	-0.072581	0.000434	0.072494	-0.073015	0.145509
24	C	-0.000017	-0.151202	0.000009	0.151185	-0.151211	0.302396
25	H	0.000021	0.100945	0.000003	-0.100924	0.100942	-0.201866
26	H	-0.000003	0.078858	0.000025	-0.078861	0.078833	-0.157694
27	H	0.000045	0.092818	-0.000006	-0.092773	0.092824	-0.185597
28	C	0.00011	-0.191841	0.000004	0.191951	-0.191845	0.383796
29	H	0.0001	0.09006	-0.000003	-0.08996	0.090063	-0.180023
30	H	0.000002	0.103748	0.000002	-0.103746	0.103746	-0.207492
31	H	0.000016	0.115915	0.000021	-0.115899	0.115894	-0.231793
32	H	0.000274	0.142442	0.000084	-0.142168	0.142358	-0.284526
33	H	0.004059	0.123157	0.003875	-0.119098	0.119282	-0.23838
34	H	-0.000603	0.110665	0.000722	-0.111268	0.109943	-0.221211
35	H	0.000226	0.147678	-0.000013	-0.147452	0.147691	-0.295143
36	H	0.000037	0.101286	-0.000005	-0.101249	0.101291	-0.20254
37	H	0.000332	0.133903	0.000234	-0.133571	0.133669	-0.26724
38	H	0.006255	0.140675	-0.001484	-0.13442	0.142159	-0.276579
39	H	-0.000449	0.107715	0.000417	-0.108164	0.107298	-0.215462

40	H	-0.028875	0.096487	-0.016503	-0.125362	0.11299	-0.238352
41	H	-0.029374	0.060726	-0.013966	-0.0901	0.074692	-0.164792
42	N	0.000368	-0.441125	0.000029	0.441493	-0.441154	0.882647
43	C	0.039038	0.082886	-0.013398	-0.043848	0.096284	-0.140132
44	C	-0.042095	0.037001	-0.021309	-0.079096	0.05831	-0.137406
45	Cl	-0.00114	0.148985	-0.00024	-0.150125	0.149225	-0.29935

Table 5. Mulliken atomic charges, Fukui function and dual descriptor of IPA by B3LYP/6-31G(d,p)

atoms		$q_k(N + 1)$	$q_k(N)$	$q_k(N - 1)$	$f_k^+$	$f_k^-$	$\Delta f_k(r)$
1	C	0.006358	-0.358103	0.014172	0.364461	-0.372275	0.736736
2	C	0.100856	0.816505	0.051931	-0.715649	<b>0.764574</b>	<b>-1.480223</b>
3	C	-0.058708	0.21258	0.134245	-0.271288	0.078335	-0.349623
4	C	-0.006053	-0.086989	0.026226	0.080936	-0.113215	0.194151
5	C	0.000353	-0.06724	-0.01243	0.067593	-0.05481	0.122403
6	C	0.034506	0.130066	-0.146647	-0.09556	0.276713	-0.372273
7	C	-0.005787	-0.045879	0.058563	0.040092	-0.104442	0.144534
8	H	0.000459	0.094941	-0.003983	-0.094482	0.098924	-0.193406
9	C	0.003548	-0.118736	-0.101259	0.122284	-0.017477	0.139761
10	C	-0.004587	-0.081435	0.072385	0.076848	-0.15382	0.230668
11	C	0.002742	-0.089221	-0.048293	0.091963	-0.040928	0.132891
12	H	0.001349	0.117077	0.003539	-0.115728	0.113538	-0.229266
13	H	0.002724	0.120748	0.000174	-0.118024	0.120574	-0.238598
14	H	0.000347	0.085476	-0.003991	-0.085129	0.089467	-0.174596
15	H	-0.000665	0.087394	0.00112	-0.088059	0.086274	-0.174333
16	H	-0.000086	0.084596	0.005109	-0.084682	0.079487	-0.164169
17	H	0.00016	0.089277	-0.002902	-0.089117	0.092179	-0.181296
18	H	0.000247	0.089692	-0.002287	-0.089445	0.091979	-0.181424
19	C	-0.071049	-0.280867	0.23085	0.209818	-0.511717	0.721535
20	C	-0.000654	-0.280546	-0.13523	0.279892	-0.145316	0.425208
21	N	0.149098	-0.462537	0.159417	<b>0.611635</b>	-0.621954	<b>1.233589</b>
22	C	-0.096977	-0.183188	-0.07647	0.086211	-0.106718	0.192929
23	C	0.134517	-0.380745	0.296894	0.515262	-0.677639	1.192901
24	C	0.174238	-0.121066	0.074121	0.295304	-0.195187	0.490491
25	C	0.113761	-0.183537	0.094685	0.297298	-0.278222	0.57552
26	H	0.003428	0.196179	-0.006423	-0.192751	0.202602	-0.395353
27	H	-0.002155	0.144291	-0.002367	-0.146446	0.146658	-0.293104
28	H	0.012611	0.135189	0.012564	-0.122578	0.122625	-0.245203
29	C	-0.002019	-0.172038	0.03045	0.170019	-0.202488	0.372507
30	H	0.001533	0.117719	-0.001713	-0.116186	0.119432	-0.235618
31	H	0.00063	0.115706	-0.000729	-0.115076	0.116435	-0.231511
32	H	0.000434	0.107897	-0.001319	-0.107463	0.109216	-0.216679

33	H	0.217488	0.223096	0.239827	-0.005608	-0.016731	0.011123
34	H	0.2714	0.114419	0.283218	0.156981	-0.168799	0.32578
35	H	-0.004773	-0.554216	0.028595	0.549443	-0.582811	1.132254
36	H	0.005055	0.204981	0.002068	-0.199926	0.202913	-0.402839
37	H	-0.017831	0.226569	0.091164	-0.2444	0.135405	-0.379805
38	H	-0.013341	0.102725	0.22038	-0.116066	-0.117655	0.001589
39	H	0.006536	0.179224	-0.0942	-0.172688	0.273424	-0.446112
40	H	0.015983	0.073512	-0.22147	-0.057529	0.294982	-0.352511
41	H	0.000641	0.17994	-0.039141	-0.179299	0.219081	-0.39838
42	H	0.009587	0.080097	-0.111155	-0.07051	0.191252	-0.261762
43	N	-0.014402	-0.495162	0.046212	0.48076	-0.541374	1.022134
44	C	0.005323	-0.108021	-0.084277	0.113344	-0.023744	0.137088
45	C	0.023173	-0.060368	-0.081624	0.083541	0.021256	0.062285

Table 6. Mulliken atomic charges, Fukui function and dual descriptor of AP by B3LYP/6-31G(d,p)

atoms	$q_k(N+1)$	$q_k(N)$	$q_k(N-1)$	$f_k^+$	$f_k^-$	$\Delta f_k(r)$	
1	C	-0.05235	-0.087875	-0.02301	0.035525	-0.064865	0.10039
2	C	0.100444	-0.118044	0.045647	0.218488	-0.163691	0.382179
3	C	0.045627	0.237435	0.017507	-0.191808	0.219928	-0.411736
4	C	0.135182	0.321394	0.052694	-0.186212	0.2687	-0.454912
5	C	-0.07906	-0.148496	-0.025322	0.069436	-0.123174	0.19261
6	C	0.211645	-0.080477	0.089308	0.292122	-0.169785	0.461907
7	C	0.006676	0.323337	0.090536	-0.316661	0.232801	-0.549462
8	C	0.00464	-0.090173	-0.072571	0.094813	-0.017602	0.112415
9	C	0.003915	-0.076915	0.279712	0.08083	-0.356627	0.437457
10	C	0.000105	-0.13143	-0.026097	0.131535	-0.105333	0.236868
11	H	0.001573	0.093451	0.00072	-0.091878	0.092731	-0.184609
12	H	-0.004942	0.106396	-0.001918	-0.111338	0.108314	-0.219652
13	H	0.002467	0.102172	0.001832	-0.099705	0.10034	-0.200045
14	H	-0.008853	0.094935	-0.00461	-0.103788	0.099545	-0.203333
15	H	0.000187	0.124735	-0.014744	-0.124548	0.139479	-0.264027
16	H	-0.000075	0.121568	-0.000211	-0.121643	0.121779	-0.243422
17	C	0.013245	0.06304	0.117069	-0.049795	-0.054029	0.004234
18	N	0.277323	-0.608977	0.088086	0.8863	-0.697063	1.583363
<b>19</b>	<b>C</b>	<b>-0.069546</b>	<b>0.488966</b>	<b>0.210246</b>	<b>-0.558512</b>	<b>0.27872</b>	<b>-0.837232</b>
20	C	0.016417	-0.035352	0.001869	0.051769	-0.037221	0.08899
21	C	0.013502	-0.327559	0.003555	0.341061	-0.331114	0.672175
22	C	-0.004836	-0.172943	0.00283	0.168107	-0.175773	0.34388
23	C	-0.008356	-0.02546	-0.000056	0.017104	-0.025404	0.042508
24	H	0.007896	0.085351	0.00098	-0.077455	0.084371	-0.161826
25	H	0.002068	0.215114	0.000001	-0.213046	0.215113	-0.428159

26	H	0.009366	0.174496	0.000098	-0.16513	0.174398	-0.339528
27	H	0.012434	0.145968	-0.000762	-0.133534	0.14673	-0.280264
28	H	0.000556	0.138025	-0.000502	-0.137469	0.138527	-0.275996
29	O	0.026118	-0.583847	-0.005964	0.609965	-0.577883	1.187848
30	N	0.081024	-0.447714	0.000142	0.528738	-0.447856	0.976594
<b>31</b>	<b>N</b>	<b>0.251982</b>	<b>-0.483167</b>	<b>0.027408</b>	<b>0.735149</b>	<b>-0.510575</b>	<b>1.245724</b>
32	Cl	0.001478	0.011692	-0.00082	-0.010214	0.012512	-0.022726
33	H	0.012176	0.160706	0.003339	-0.14853	0.157367	-0.305897
34	H	-0.001232	0.099037	0.000495	-0.100269	0.098542	-0.198811
35	H	-0.00031	0.137652	0.001134	-0.137962	0.136518	-0.27448
36	H	0.000102	0.174697	-0.00096	-0.174595	0.175657	-0.350252
37	C	-0.008767	-0.187205	0.14943	0.178438	-0.336635	0.515073
38	H	0.000178	0.185467	-0.007093	-0.185289	0.19256	-0.377849

Table 7. Mulliken atomic charges, Fukui function and dual descriptor of IZ by B3LYP/6-31G(d,p)

atoms	$q_k(N+1)$	$q_k(N)$	$q_k(N-1)$	$f_k^+$	$f_k^-$	$\Delta f_k(r)$	
1	C	0.043	0.123456	0.032069	-0.080456	0.091387	-0.171843
2	C	0.060373	-0.147992	0.069159	0.208365	-0.217151	0.425516
3	C	-0.028729	0.079073	0.279278	-0.107802	-0.200205	0.092403
4	C	0.066344	-0.098964	0.109006	0.165308	-0.20797	0.373278
5	C	0.039367	0.068222	-0.018675	-0.028855	0.086897	-0.115752
6	H	0.005949	0.120136	-0.003714	-0.114187	0.12385	-0.238037
7	H	0.000087	0.125399	-0.004621	-0.125312	0.13002	-0.255332
8	H	0.000582	0.112058	-0.006495	-0.111476	0.118553	-0.230029
9	H	0.003651	0.117903	-0.000954	-0.114252	0.118857	-0.233109
<b>10</b>	<b>N</b>	<b>0.206367</b>	<b>-0.430326</b>	<b>0.280544</b>	<b>0.636693</b>	<b>-0.71087</b>	<b>1.347563</b>
<b>11</b>	<b>C</b>	<b>-0.019574</b>	<b>0.511062</b>	<b>0.12105</b>	<b>-0.530636</b>	<b>0.390012</b>	<b>-0.920648</b>
12	N	0.080939	-0.427799	0.020945	0.508738	-0.448744	0.957482
13	N	0.375402	-0.254347	-0.002068	0.629749	-0.252279	0.882028
14	C	-0.005029	0.046981	0.003057	-0.05201	0.043924	-0.095934
15	C	0.001981	-0.318967	0.001628	0.320948	-0.320595	0.641543
16	H	-0.000448	0.108788	-0.000025	-0.109236	0.108813	-0.218049
17	H	0.003272	0.126298	-0.000029	-0.123026	0.126327	-0.249353
18	H	0.000432	0.099489	0.000196	-0.099057	0.099293	-0.19835
19	C	0.025604	-0.294461	-0.000083	0.320065	-0.294378	0.614443
20	H	0.002278	0.118166	0.00022	-0.115888	0.117946	-0.233834
21	H	0.000681	0.096638	0.000006	-0.095957	0.096632	-0.192589
22	H	-0.001382	0.112247	-0.000099	-0.113629	0.112346	-0.225975
23	H	0.049476	0.066631	-0.000182	-0.017155	0.066813	-0.083968
24	H	0.006834	0.255033	-0.000856	-0.248199	0.255889	-0.504088
25	H	0.009924	0.248905	0.003139	-0.238981	0.245766	-0.484747
26	O	0.072617	-0.463628	0.117505	0.536245	-0.581133	1.117378

#### 4. Conclusion

Density functional theory at B3LYP/6-31G(d,p) level was used to obtain theoretical insight into the inhibition effect of clomipramine, Imipramine, Amoxapine and Iproniazid in metal corrosion in acidic solution.

Global reactivity parameters such as highest occupied molecular orbital energy ( $E_{\text{HOMO}}$ ), the lowest unoccupied molecular orbital energy ( $E_{\text{LUMO}}$ ), electrophilicity index ( $\omega$ ), fraction of electrons transferred ( $\Delta N$ ) and electronegativity ( $\chi$ ) have clarified the electronic interactions of studied molecules with the atoms of considered metals. These interactions give them good inhibition potentialities. Moreover the values of energy gap ( $\Delta E$ ), the electronegativity ( $\chi$ ), the hardness ( $\eta$ ) and the softness ( $\sigma$ ) attest that these molecules are strongly reactive, so these compounds can easily adsorb to metal surface. As for electroaccepting power parameter ( $\omega^+$ ) values of CPA, IPA and IZ mentions that these three compounds have good ability to accept electrons from metal, then according to the electrodonating power ( $\omega^-$ ) values, AP has strong performance to donate electrons to metal. It has been found that the presence of certain constituents on studied compounds influences their ability to donate or to receive electrons. The probable electrophilic and nucleophilic attack sites of each compound were identified through the local parameters. Ultimately although these molecules help to combat depression, they can also be used to inhibit iron, copper and aluminum corrosion in acidic solutions.

#### References

- Abd El-Maksoud, S. A., El-Dossoki, F. I., Migahed, M. A., Gouda, M. M., & El-Sayed, R. H. E. (2021). New Imidazol-1-ium Bromide Derivative Surfactants as Corrosion Inhibitors for Carbon Steel in 1 M HCl Solutions: Experimental and Theoretical Studies. *Journal of Bio-and Tribo-Corrosion*, 7, 156 <https://doi.org/10.1007/s40735-021-00595-4>
- Adejoro, I. A., Akintayo, D. C., & Ibeji, C. U. (2016). The efficiency of chloroquine as corrosion inhibitor for Aluminium in 1M HCl: Experimental and DFT study. *Jordan Journal of Chemistry*, 11(1), 38-49.
- Albayati, M. R., Kansız, S., Dege, N., Savaş, K., Marzouki, R., Lgaz, H., ... & Chung Ill., M. (2020). Synthesis, crystal structure, Hirshfeld surface analysis and DFT calculations of 2-[(2,3-dimethylphenyl)amino]-N'-[(E)-thiophen-2-ylmethylidene]benzohydrazide, *Journal of Molecular Structure* (2020). *Journal of Molecular Structure*, 1205, 127654. <https://doi.org/10.1016/j.molstruc.2019.127654>
- Ambrish, S., Ansari, K. R., Jiyaul, H., Parul D., Hassane, L., Rachid, S., & Quraishi, M. A. (2018). Effect of electron donating functional groups on corrosion inhibition of mild steel in hydrochloric acid: Experimental and quantum chemical study. *Journal of the Taiwan Institute of Chemical Engineers*, 82, 233-251. <https://doi.org/10.1016/j.jtice.2017.09.021>
- Bahlakeh, G., Ramezanzadeh, B., Dehghani, A., & Ramezanzadeh M. (2019). Novel cost-effective and high-performance green inhibitor based on aqueous Peganum harmala seed extract for mild steel corrosion in HCl solution: detailed experimental and electronic/atomic level computational explorations. *Journal of Molecular Liquids*, 283, 174-195. <https://doi.org/10.1016/j.molliq.2019.03.086>
- Becke, A. D. (1992). Density-functional thermochemistry. I. The effect of the exchange-only gradient correction. *The Journal of Chemical Physics*, 96, 2155-2160. <https://doi.org/10.1063/1.462066>
- Behzadi, H., Roonasi, P., Momeni, M. J., Manzetti, S., Esrafil, M. D., Obot, I. B., Yousefvand, M., & Morteza Mousavi-Khoshdel, S. (2015). A DFT study of pyrazine derivatives and their Fe complexes in corrosion inhibition process. *Journal of Molecular Structure*, 1086, 64-72. <https://doi.org/10.1016/j.molstruc.2015.01.008>
- Bochuan, T., Shengtao, Z., Yujie, Q., Lei, G., Li, F., Chaohui, L., Yue, X., & Shijin, C. (2018). A combined experimental and theoretical study of the inhibition effect of three disulfide-based flavouring agents for copper corrosion in 0.5 M sulfuric acid. *Journal of Colloid and Interface Science*, 526, 268-280. <https://doi.org/10.1016/j.jcis.2018.04.092>
- Cher, T. S., Petar, Ž., & Ming, W. W. (2020). Prediction of corrosion inhibition efficiency of pyridines and quinolines on an iron surface using machine learning-powered quantitative structure-property relationships. *Applied Surface Science*, 512, 145612. <https://doi.org/10.1016/j.apsusc.2020.145612>
- Danaee, I., Ghasemi, O., Rashed, G. R., Rashvand, A., & Maddahy, M. H. (2013). Effect of hydroxyl group position on adsorption behavior and corrosion inhibition of hydroxybenzaldehyde Schiff bases: Electrochemical and quantum calculations. *Journal of Molecular Structure*, 1035, 247-259. <https://doi.org/10.1016/j.molstruc.2012.11.013>
- Dehghani, A., Bahlakeh, G., Ramezanzadeh, B., & Ramezanzadeh, M. (2019). A combined experimental and theoretical study of green corrosion inhibition of mild steel in HCl solution by aqueous Citrullus lanatus fruit (CLF) extract. *Journal of Molecular Liquids*, 279, 603-624. <https://doi.org/10.1016/j.molliq.2019.02.010>

- Dehghani, A., Mostafatabar, A., Bahlakeh, G., Ramezanzadeh, B., & Ramezanzadeh, M. (2019). Detailed-level computer modeling explorations complemented with comprehensive experimental studies of Quercetin as a highly effective inhibitor for acid-induced steel corrosion. *Journal of Molecular Liquids*, 283, 174-195. <https://doi.org/10.1016/j.molliq.2019.03.086>
- Dewar, M. J. S., Zebisch, E. G., Healy, E. F., & Stewart, J. P. (1985). Development and use of quantum mechanical molecular models. 76. AM1: a new general purpose quantum mechanical molecular model. *Journal of the American Chemical Society*, 107(13), 3902- 3909. <https://doi.org/10.1021/ja00299a024>
- Frisch, M. J., Trucks, G. W., Schlegel, H. B., et al. (2009). Gaussian 09. Gaussian, Inc., Wallingford
- Hohenberg, P., & Kohn, W. (1964). Inhomogeneous electron gas. *Physical Review*, 136, B864-B887. <https://doi.org/10.1103/PhysRev.136.B864>
- Ileana, R., Simona, V., Luiza, G., & Liana, M. M. (2014). Antibacterial drugs as corrosion inhibitors for bronze surfaces in acidic solutions. *Applied Surface Science*, 321, 188-196, <https://doi.org/10.1016/j.apsusc.2014.09.201>
- Jabir, H., Al-Fahemi, Abdallah, M., Elshafie, M., Gad, A. M. L., & Jahdaly, B. A. A. (2016). Experimental and theoretical approach studies for melatonin drug as safely corrosion inhibitors for carbon steel using DFT. *Journal of Molecular Liquids*, 222, 1157-1163, <https://doi.org/10.1016/j.molliq.2016.07.085>
- Jian, Z., Wenpo, L., Xiuli, Z., Yanyun, C., Wei, L., Yu, Z., Anqing, F., Bochuan, T., & Shengtao, Z. (2018). Combining experiment and theory researches to insight into anticorrosion nature of a novel thiazole derivative. *Journal of the Taiwan Institute of Chemical Engineers*, 122, 190-200. <https://doi.org/10.1016/j.tjice.2021.04.035>
- Jing, Z., Zheng, L., Guo-Cheng, H., ShiLiang, C., & Zhencheng, C. (2016). Inhibition of copper corrosion by the formation of Schiff base self-assembled monolayers. *Applied Surface Science*, 389, 601-608 <http://dx.doi.org/10.1016/j.apsusc.2016.07.116>
- José, L. Gázquez, J. L., Cedillo, A., & Vela A. (2007). Electrodonating and electroaccepting powers. *The Journal of Physical Chemistry*, 111, 1966-1970. <https://doi.org/10.1021/jp065459f>
- Khaled, K. F. (2008). Adsorption and inhibitive properties of a new synthesized guanidine derivative on corrosion of copper in 0.5 M H<sub>2</sub>SO<sub>4</sub>. *Applied Surface Science*, 255, 1811-1818. <https://doi.org/10.1016/j.apsusc.2008.06.030>
- Khattabi, M., Benhiba, F., Tabti, S., Djedouani, A., El Assyry, A., Touzani, R., ... & Zarrouk, A. (2019). Performance and computational studies of two soluble pyran derivatives as corrosion inhibitors for mild steel in HCl. *Journal of Molecular Structure*, 1196, 231-244. <https://doi.org/10.1016/j.molstruc.2019.06.070>
- Kurks, E., Anwera, A. A., Faragb, E. A., Mohamed, E. M., & Azmyc, G. H. (2021). Sayeda. Corrosion inhibition performance and computational studies of pyridine and pyran derivatives for API X-65 steel in 6 M H<sub>2</sub>SO<sub>4</sub>. *Journal of Industrial and Engineering Chemistry*, 97, 523-538. <https://doi.org/10.1016/j.jiec.2021.03.016>
- Lanzhou, G., Shini, P., Xiaomei, H., & Zhili, G. (2020). A combined experimental and theoretical study of papain as a biological eco-friendly inhibitor for copper corrosion in H<sub>2</sub>SO<sub>4</sub> medium. *Applied Surface Science*, 511, 145446, <https://doi.org/10.1016/j.apsusc.2020.145446>
- Lazrak, E., Ech-chihbi, B., El Ibrahim, F., El Hajjaji, Z., Rais, M., & Tachihante, M. T. (2022). Detailed DFT/MD simulation, surface analysis and electrochemical computer explorations of aldehyde derivatives for mild steel in 1.0 M HCl. *Colloids and Surfaces A: Physicochemical and Engineering Aspects*, 632, 127822. <https://doi.org/10.1016/j.colsurfa.2021.127822>
- Lee, C., Yang, W., & Parr, R. G. (1988). Development of the Colle-Salvetti correlation-energy formula into a functional of the electron density. *Physical Review B*, 37, 785-789. <https://doi.org/10.1103/PhysRevB.37.785>
- Lianjun, H., Guofeng, P., Hao, W., Yi, X., & Ru, W. (2020). The synergistic inhibitory effect and density functional theory study of 2,2'-[(Methyl-1H-benzotriazol-1-yl)methyl]imino]bisethanol and potassium oleate on copper in H<sub>2</sub>O<sub>2</sub> based alkaline slurries. *Colloids and Surfaces A: Physicochemical and Engineering*, 603, 125275. <https://doi.org/10.1016/j.colsurfa.2020.125275>
- Loganathan, K. T., Venkatesan, S. T., Nagarajan, S., & Natarajan, R. (2021). Corrosion inhibitive evaluation and DFT studies of 2-(Furan-2-yl)-4,5-diphenyl-1H-imidazole on mild steel at 1.0M HCl. *Journal of the Indian Chemical Society*, 98(9), 100121. <https://doi.org/10.1016/j.jics.2021.100121>
- Lukman, O. O., Mwacham, M. K., & Eno, E. E. (2016). Quinoxaline derivatives as corrosion inhibitors for mild steel in hydrochloric acid medium: Electrochemical and quantum chemical studies. *Physica E: Low-dimensional Systems and Nanostructures*, 76, 109-126. <https://doi.org/10.1016/j.physe.2015.10.005>

- Martínez-Araya, J. I. (2015). Why is the dual descriptor a more accurate local reactivity descriptor than Fukui functions? *Journal of Mathematical Chemistry*, 5, 451-465. <https://doi.org/10.1007/s10910-014-0437-7>
- Maryam, C., Abdelkarim, C., Hassane, L., Rachid, S., Vijaya, B. K., Riadh, M., ... & Ill-Min, C. (2020). Inhibition performances of spirocyclopropane derivatives for mild steel protection in HCl. *Materials Chemistry and Physics*, 243, 122582. <https://doi.org/10.1016/j.matchemphys.2019.122582>
- Michaelson, H. B. (1977). The work function of the elements and its periodicity. *Journal of Applied Physics*, 48, 4729-4733. <https://doi.org/10.1063/1.323539>
- Mohanapriya, N., Kumaravel, M., & Lalithamani, B. (2020). Theoretical and Experimental Studies on the Adsorption of N- [(E)-Pyridin-2-ylmethylidene] Aniline, a Schiff Base, on Mild Steel Surface in Acid Media. *Journal of Electrochemical Science and Technology*, 11(2), 117-131. <https://doi.org/10.33961/jecst.2019.00430>
- Morell, C., Grand, A., & Toro-Labbé, A. (2005). New dual descriptor for chemical reactivity. *Journal of Physical Chemistry A*, 109(1), 205-212. <https://doi.org/10.1021/jp046577a>
- Nurudeen, A. O., Mohammad, A. J. M., & Shaikh, A. A. (2022). Tipping Effect of Tetra-alkylammonium on the Potency of N-(6-(1H-benzo[d]imidazol-1-yl)hexyl)-N, N-dimethyldodecan-1-aminium bromide (BIDAB) as Corrosion Inhibitor of Austenitic 304L Stainless Steel in Oil and Gas Acidization: Experimental and DFT Approach. *Journal of Molecular Liquids*, 55, 119431. <https://doi.org/10.1016/j.molliq.2022.119431>
- Palaniappan, N., Alphonsa, J., Cole, I. S., Balasubramanian, K., & Bosco, I. G. (2019). Rapid investigation expiry drug green corrosion inhibitor on mild steel in NaCl medium. *Materials Science and Engineering: B*, 249, 114423, <https://doi.org/10.1016/j.mseb.2019.114423>
- Parr, R. G., Sventpaly, L., & Liu, S. (1999). Electrophilicity index. *Journal of the American Chemical Society*, 121(9), 1922-1924. <https://doi.org/10.1021/ja983494x>
- Pavithra, M. K.; Venkatesha, T. V., & Punith Kumar, M. K. (2013). Inhibiting Effects of Rabeprazole Sulfide on the Corrosion of Mild Steel in Acidic Chloride Solution. *International Journal of Electrochemistry*, 1-9. <https://doi.org/10.1155/2013/714372>
- Pearson, R. G. (1988). Absolute Electronegativity and Hardness: application to Inorganic Chemistry. *Inorganic Chemistry*, 27 (4), 734-740. <https://doi.org/10.1021/ic00277a030>
- Priyanka, S., Ambrish, S., Quraishi, M. A. (2016). Thiopyrimidine derivatives as new and effective corrosion inhibitors for mild steel in hydrochloric acid: Electrochemical and quantum chemical studies. *Journal of the Taiwan Institute of Chemical*, 60, 588-601. <https://doi.org/10.1016/j.jtice.2015.10.033>
- Rahmani, H., Alaoui, K. I., EL Azzouzi, M., Benhiba, F., El Hallaoui, A., Rais, Z., ... & Zarrouk, A. (2019). Corrosion assessment of mild steel in acid environment using novel triazole derivative as an anti-corrosion agent: A combined experimental and quantum chemical study. *Chemical Data Collections*, 24, 100302, <https://doi.org/10.1016/j.cdc.2019.100302>.
- Rajesh, H., Dwarika, P., Akhil, S., & Raman, K. (2018). Experimental and theoretical studies of Ficus religiosa as green corrosion inhibitor for mild steel in 0.5 M H<sub>2</sub>SO<sub>4</sub> solution. *Sustainable Chemistry and Pharmacy*, 9, 95-105. <https://doi.org/10.1016/j.scp.2018.07.002>
- Soltani, N., Behpour, M., Oguzie, E. E., Mahluji, M., & Ghasemzadeh, M. A. (2015). Pyrimidine-2-thione Derivatives as Corrosion Inhibitors for Mild Steel in Acidic Environments. *Royal society of chemistry Advances*, 5, 11145-11162.
- Sourav K. S., Pritam, G., Abhiram, H., Naresh, C. M., & Priyabrata, B. (2015). Density functional theory and molecular dynamics simulation study on corrosion inhibition performance of mild steel by mercapto-quinoline Schiff base corrosion inhibitor. *Physica E: Low-dimensional Systems and Nanostructures*, 66, 332-341. <https://doi.org/10.1016/j.physe.2014.10.035>
- Sumayah, B., Vivek S., Hassane, L., Ill-Min C., Ambrish, S., & Ashish, K. (2018). The inhibition action of analgin on the corrosion of mild steel in acidic medium: A combined theoretical and experimental approach. *Journal of Molecular Liquids*, 263, 454-462. <https://doi.org/10.1016/j.molliq.2018.04.143>
- Tengda, M., Baimei, T., Lei, G., Savas, K., Zhengxiao, K., Shihao, Z., ... & Yangang, H. (2021). Multidimensional insights into the corrosion inhibition of potassium oleate on Cu in alkaline medium: A combined Experimental and theoretical investigation. *Materials Science and Engineering*, 272, 115330. <https://doi.org/10.1016/j.mseb.2021.115330>
- Tigori, A. M., Koné, A., Souleymane, B., Zon, D., Sissouma, D., & Marius Niamien, P. M. (2022). Combining

- Experimental and Quantum Chemical Study of 2-(5-Nitro-1,3-Dihydro Benzimidazol-2-Ylidene)-3-Oxo-3-(2-Oxo-2H-Chromen-3-yl) Propanenitrile as Copper Corrosion Inhibitor in Nitric Acid Solution. *Open Journal of Physical Chemistry*, 12, 47-70. <https://doi.org/10.4236/ojpc.2022.124004>.
- Vandana, S., Mahendra, Y., & Obot, I. B. (2020). Investigations on eco-friendly corrosion inhibitors for mild steel in acid environment: Electrochemical, DFT and Monte Carlo Simulation approach. *Colloids and Surfaces A: Physicochemical and Engineering Aspects*, 599, 124881. <https://doi.org/10.1016/j.colsurfa.2020.124881>
- Vranda, S. K., Pushyaraga, P. V., Kumari, R. P. D., & Debashree, C.(2021). Effective inhibition of mild steel corrosion by 6-bromo-(2,4-dimethoxyphenyl)methylidene]imidazo [1,2-a]pyridine-2-carbohydrazide in 0.5 M HCl: Insights from experimental and computational study. *Journal of Molecular Structure*, 1232, 130074. <https://doi.org/10.1016/j.molstruc.2021.130074>
- Yue, X., Shengtao, Z., Wenpo, L., Lei, G., Shenying, X., Li, F., & Loutfy, H. M. (2018). Experimental and theoretical examinations of two quinolin-8-ol-piperazine derivatives as organic corrosion inhibitors for C35E steel in hydrochloric acid. *Applied Surface Science*, 459, 612-620, <https://doi.org/10.1016/j.apsusc.2022.118900>
- Žaklina, Z. T., Marija, B., Petrović, M., Milan, B. R., & Milan, M. (2018). Antonijević Electrochemical Investigations of Copper Corrosion Inhibition by Azithromycin in 0.9% NaCl. *Journal of Molecular Liquids*, 265, 687-692. <https://doi.org/10.1016/j.molliq.2018.03.11>
- Žaklina, Z., TasićMarija, B., Mihajlović, P., Radovanović, M. B., Simonović, A. T., & Antonijević, M. M.(2021). Experimental and theoretical studies of paracetamol as a copper corrosion inhibitor. *Journal of Molecular Liquids*, 327, 114817, 1-9. <https://doi.org/10.1016/j.molliq.2020.114817>
- Zarrouk, A., El Ouali, I., Bouachrine, M., Hammouti, B., Ramli, Y., Essassi, E. M., ... & Salghi, R. (2013). Theoretical approach to the corrosion inhibition efficiency of some quinoxaline derivatives of steel in acid media using the DFT method. *Research on Chemical Intermediates*, 39(3), 1125-1133. <https://doi.org/10.1007/s11164-012-0671-1>
- Zarrouk, A., Hammouti, B., Ali, D., Mohammed, B., Hassan, Z., Boukhris, S., & Salem, S. A. (2014). A theoretical study on the inhibition efficiencies of some quinoxalines as corrosion inhibitors of copper in nitric acid. *Journal of Saudi Chemical Society*, 18, 450-55. <http://dx.doi.org/10.1016/j.jscs.2011.09.011>
- Zhang, J., Li, W., Zuo, X., Chen, Y., Luo, W., Zhang, Y., Fu, A., Tan, B., & Zhang, S. (2021). Combining Experiment and Theory Researches to Insight into Anticorrosion Nature of a Novel Thiazole Derivative. *Journal of the Taiwan Institute of Chemical Engineers*, 122, 190-200. <https://doi.org/10.1016/j.jtice.2021.04.035>
- Ziegler, T. (1991). Approximate Density Functional Theory as a Practical tool in molecular in molecular Energetics and dynamics. *Chemical Review*, 91, 651-667

## Copyrights

Copyright for this article is retained by the author(s), with first publication rights granted to the journal.

This is an open-access article distributed under the terms and conditions of the Creative Commons Attribution license (<http://creativecommons.org/licenses/by/4.0/>).